

# NEAR-FIELD CHARACTERIZATION OF RECONFIGURABLE NARROWBAND ANTENNA IN THE PROXIMITY OF HUMAN BODY

Ibrahim Elshafiey<sup>1</sup>, Abdel-Fattah Sheta<sup>1</sup>, Majeed A. Alkanha<sup>1</sup>, Ashraf Mohra<sup>1</sup>, and Abdullah AlOrainy<sup>2</sup>

<sup>1</sup>Advanced Technologies Research Center (ATRC), Dept. of Electrical Engineering, King Saud University, P. O. Box 800, Riyadh 11421, Saudi Arabia

<sup>2</sup>Electronics Research Institute, King Abdulaziz City for Science and Technology, Riyadh, Saudi Arabia

**ABSTRACT.** Reconfigurable antennas have been suggested recently for use in various mobile systems. These systems are usually operated in the vicinity of human body, leading to mutual interaction with body tissues. A nondestructive evaluation method is developed to characterize a reconfigurable antenna designed to cover the GSM-900/DCS-1800 bands. Modeling based on FDTD is performed of the antenna in free space and in proximity to human head. Results reveal frequency shift, and variations in the matching and bandwidth, depending on antenna orientation with respect to the head. Experimental setup is also used to characterize the SAR values in human head. A six-degree-of-freedom robot is implemented to scan a head phantom using specialized sensors and head simulating liquids. The developed system provides a tool for guiding the design of the new category of reconfigurable antennas.

**Keywords:** Reconfigurable Antenna, SAR, FDTD

**PACS:** 84.40.Ba, 87.50.cm, 02.70.Bf

## INTRODUCTION

Future wireless communication systems must support multiple radio standards. RF circuit design should offer flexibility and programmability. Antenna composes an essential element in modern communication system. Reconfigurable antennas have been introduced recently for various applications including mobile communication devices. These devices are usually operated near the human body, leading to mutual interaction between the RF system and the body tissues. The relatively high values of permittivity of human tissues affect the antenna radiation characteristics as well as its operating frequency. The wave velocity is also decreased inside the tissue according to tissue parameters. Tissue parameters however vary considerably. The relative permittivity  $\epsilon_r$  is high in water rich tissues such as liver and low in other tissues such as fat or bone. Even one tissue type such as nervous tissues in brain exhibits considerable differences between gray matter and white matter.

Induced currents in the tissues constitute part of the radiating element and thus affect the radiation characteristics. The tissues also absorb part of the RF power, which should be characterized accurately to assure compliance with standards related to dose limits. Most countries have set guidelines that limit the significant thermal effects of RF radiation. A nondestructive evaluation method is presented to characterize the interaction of reconfigurable antenna with human body using computational and experimental techniques.

## **DUAL-BAND MICROSTRIP ANTENNA**

The limited space for the antenna module in mobile handset imposes the use of light weight, and small size antennas. Microstrip antennas are the best type to satisfy these requirements. Small size antennas usually suffer from bandwidth limitations. However, bandwidth can be increased either by increasing the antenna height such as PIFA structure or by adding lossy elements. Use of lossy elements, however, has negative effects on the efficiency of the antenna. Recently, reconfigurable antennas were proposed to solve the bandwidth limitation problem [1]. The concept of this type of antennas is based on tuning the antenna to achieve the desired band. The resultant tunable structure does not cover all the bands simultaneously, but provides dynamically selectable narrow instantaneous bandwidths, with efficiency higher than conventional designs [2] and [3]. Reconfigurable antennas can be implemented using microstrip structure reactively loaded with either varactor diodes (controllable capacitors) [4-7], or antenna switches (PIN diodes). This allows control of the instantaneous resonance frequency [8-10].

With the emergence of reconfigurable antennas for mobile handsets, it is essential to investigate the new structure in order to meet the technical requirements of integrating such antennas in mobile devices. The effect of presence of human head on antenna characteristics is an important issue. Another aspect is concerned with the interaction of these antennas with human tissues. Public concerns however have been expressed over the possibility that RF fields can cause non-thermal biological and health effects, at levels below those known to cause thermal effects [11]. Low RF dosimetry is added as a technical challenge to the list of performance parameters.

This paper investigates a recently published reconfigurable dual band antenna, proposed by some of the authors [2]. The investigation includes computational modeling and experimental validation of the interaction of such antenna with the human head.

## **ANTENNA STRUCTURE**

The designed antenna consists of two resonant elements: an inverted large L-shape element that resonates at the lower frequency, 900 MHz, and another smaller L-shape element that resonates at the higher frequency, 1800 MHz. Each element is designed separately and then integrated as shown in Fig. 1. The integration is achieved such that the location of the shorting post and the feeder, for each separate element, does not change. The antenna is designed on a foam substrate with thickness 2.44 mm and dielectric constant 1.2. The design parameters of the antenna are first calculated to resonate at the far ends of the two bands GSM900 and DCS1800, 960 MHz and 1880 MHz. After that, the effect of varactor loading is estimated and compensated in the antenna dimensions to allow control of the entire operating bands. The short circuited post and the feeder are located very close to each other for the matching purpose. Their radii are the same and equal 0.5 mm. The effect of loading the antenna by varactor diodes at the open ends is studied in [2].

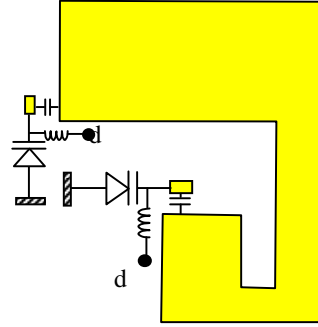


**FIGURE 1.** Dual-band varactor-based reconfigurable antenna under investigation.

## HEALTH EFFECTS OF RADIO FREQUENCY RADIATION

For temperature elevation below 0.1 °C RF radiation could be considered physiologically and biologically insignificant [11]. Exposure limits are given in terms of the specific absorption rate (SAR) to limit temperature increase in the human tissues. A number of studies also considered non-thermal effects [12] and [13]. SAR defines the absorbed dose rate and it is thus the time derivative of the incremental energy absorbed by or dissipated in an incremental mass, which given as:

$$SAR = \frac{d}{dt} \left( \frac{dW}{dm} \right) = \frac{d}{dt} \left( \frac{dW}{\rho dv} \right) \quad (1)$$

Where  $m$  is the mass,  $v$  is the volume and  $\rho$  is the density.

One way of determining the SAR is by measuring the electric field ( $E$ ) inside the tissue-simulating material. SAR will be given in terms of conductivity  $\sigma$  and density  $\rho$  as

$$SAR = \frac{\sigma |E|^2}{\rho} \quad (2)$$

## COMPUTATIONAL MODELLING

Simulation is performed using Finite-Different Time-Domain FDTD technique. FDTD has gained wide interest since it was introduced by Yee in 1966 [14]. The model is built under SEMCAD-X environment: a 3-D full wave simulation package developed by Schmid & Partner Engineering (SPEAG) [15]. The software is designed to address the electromagnetic aspects of the wireless and medical sectors in terms of antenna design, electromagnetic compatibility EMC and dosimetry. Electrical parameters of different body tissues, known as the Gabriel parameters are included in the package [16].

The antenna is first studied in free space and then close to a numerical phantom of the human head. A phantom called Specific Anthropomorphic Mannequin (SAM) is used as shown in Figure 2, with the antenna next to the left ear of SAM. The relative permittivity  $\epsilon_r$  of the tissue simulating liquid is taken as 41.5 whereas the shell is modeled as  $\epsilon_r = 3.7$ . The conductivity of the liquid is taken to be 0.97 S/m. The distance between the antenna and the ear is 0.5 mm. The previously indicated foam parameters are used for the substrate of antenna, and the copper parts are modeled by a resistive sheet of 30  $\mu\text{m}$  thickness.

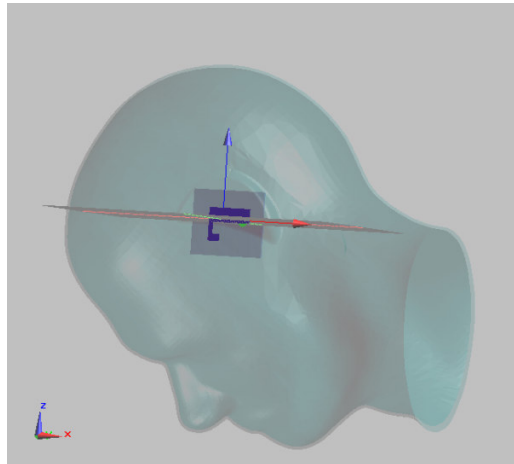


**FIGURE 2.** Antenna next to left ear of SAM model.

The varactor connected to the end of the large patch is simulated with a lumped capacitor element of 1.45 pF. The smaller patch, antenna element designed to operate at 1800 MHz band, associated varactor is modeled with a lower value capacitor of 0.5 pF to shift the second resonance frequency of typically 1800 MHz to higher frequency range.

## **EXPERIMENTAL SETUP**

The experimental setup is based on DASY-5 system manufactured by SPEAG [17]. The system implements six-degree-of-freedom robot, head phantom, measurement sensors and head simulating liquids. SAM phantom is used in the system. It is filled with human brain simulating liquid corresponding to the tissue parameters at the frequency of interest. SAM incorporates a lossless simulated ear. SAR probes specially designed for use in liquids with high permittivity values are used. The probes are calibrated in various liquids corresponding to different frequencies.

## **COMPUTATIONAL MODELING RESULTS**

Analysis is presented here using broadband simulation with center frequency of 900 MHz and bandwidth of 300-MHz. Simulation time is taken to be 250 cycles to assure achieving steady state solution.

Figure 3 presents the simulated values of  $S_{11}$  parameters corresponding to loaded and unloaded antennas with human simulating tissues. The loaded antenna reveals a shift in center frequency of around 10 MHz. There is also a considerable increase in bandwidth, which is obviously associated with increase of losses in the tissue simulating liquid.

The current distributions at 880 MHz on the surface of the antenna and the ground plane are presented in Figures 4. The figure reveals that current is high around the feeder and the shorting post on both planes. The figures also reveal that the current is mainly concentrated in the narrower branch.

Figure 5 presents the far field radiation pattern at 880 MHz of the antenna in loaded and unloaded cases. Significant deformation in the antenna radiation pattern is noticed as a result of the interaction with the head. Figure 6 presents SAR distribution calculated per 1-gram of tissue mass on a slice that is 5-mm away from the antenna surface inside the head. The input power delivered to the antenna in this case is 10-mW.

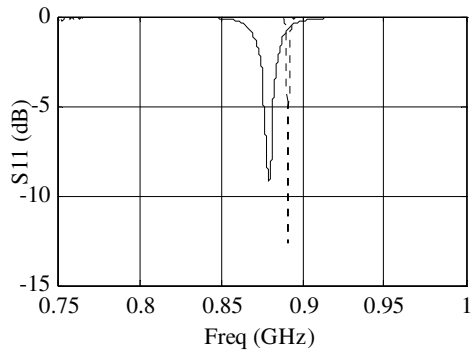


**FIGURE 3.** Effect of human head model on the reflection coefficient of the reconfigurable antenna. The dotted line is for antenna in free space, while the solid line for the antenna close to human head.

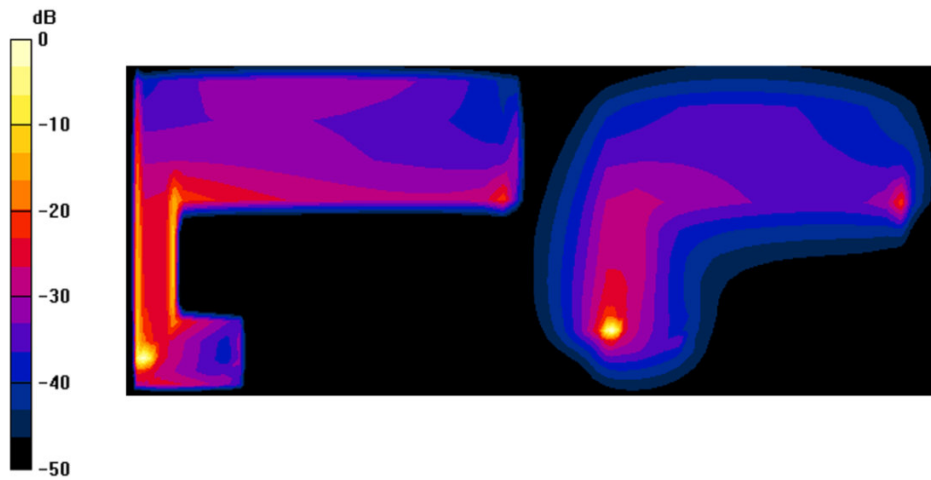


**FIGURE 4.** Current distribution on the antenna structure (left) and ground plane (right). 0-dB corresponds to  $8144 \text{ A/m}^2$ .

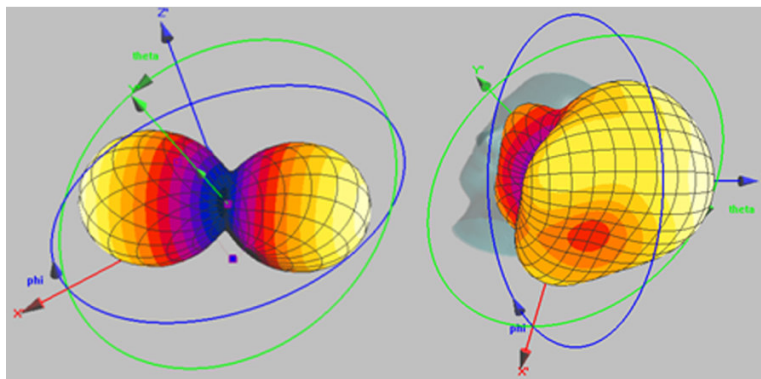


**FIGURE 5.** Radiation pattern of unloaded antenna (left), and of the loaded antenna close to the human head (right).

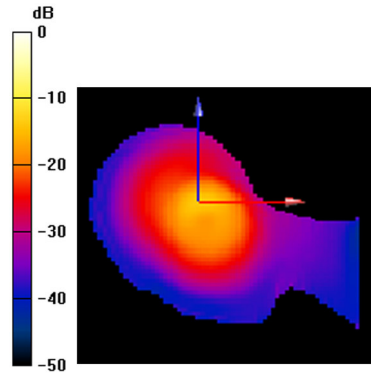


**FIGURE 6.** SAR distribution in a cross section in the head 5-mm from the antenna. 0-dB corresponds to 0.031mW/g

## EXPERIMENTAL RESULTS

The reconfigurable antenna designed and characterized using computational modeling in the previous sections is experimentally tested. First, the antenna is measured using Anritsu vector network analyzer (VNA) to study the effect of human head on impedance matching. Two types of simulating liquids human head are used. The first one is the liquid that simulates the human head parameters at 900 MHz (HSL-900), while the second is the liquid simulating the human head at 1800 MHz (HSL-1800). Figures 7 and 8 present the effect of human head simulating liquids HSL-900 and HSL-1800 on  $S_{11}$ . Significant frequency shift is observed if the antenna patch is faced to human head (front loading). The frequency shift is about 48 MHz in the GSM-900 band and about 35 MHz in the DCS-1800 band when using HSL-900. This shift is reduced to 35 MHz in the GSM-900 band and 23 MHz in the DCS-1800 band when using HSL-1800.

Simulating liquids can be used to predict the effect of human head on impedance matching experimentally, with good accuracy. The effect of front loading on antenna bandwidth, measured for 10-dB return loss, is increased from 12 MHz in the GSM-900 band to about 18 MHz for both liquids. At the DCS-1800 band, the bandwidth increases from 35 MHz to about 70 MHz for both simulating liquids. Almost no changes in bandwidth are remarked in the case of back loading with the antenna ground positioned facing the human head.

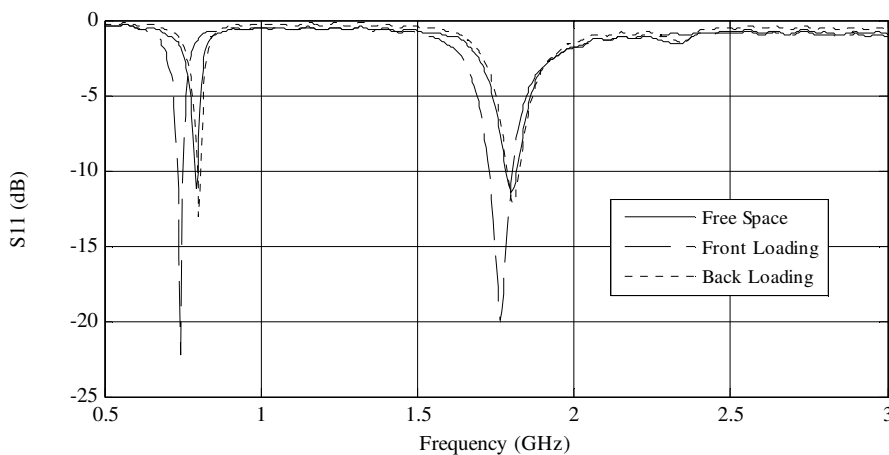


**FIGURE 7.** Experimental results of  $S_{11}$  for the reconfigurable antenna in free space and in the vicinity of human head. HSL-900 is used to simulated human head and antenna is set in two positions: patch is facing the liquid (front loading) and ground is facing the liquid (back loading).

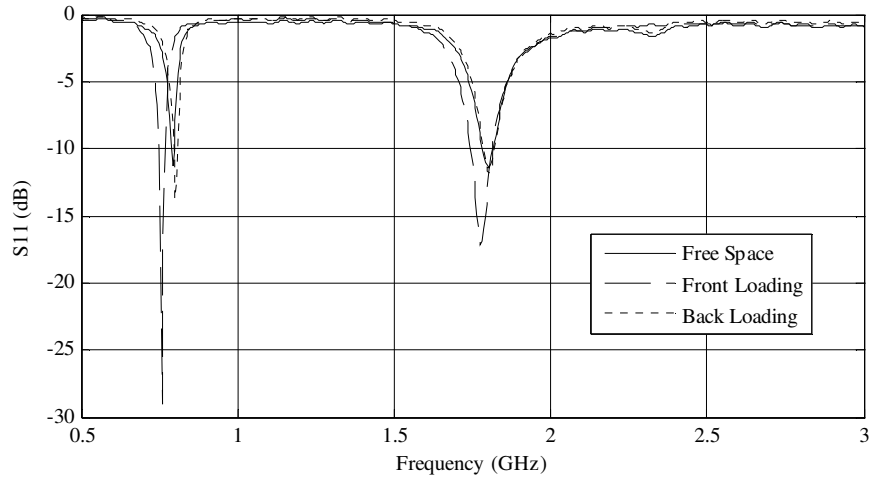


**FIGURE 8.** Experimental results of  $S_{11}$  for the reconfigurable antenna in free space and in the vicinity of human head. HSL-1800 is used to simulated human head and antenna is set in two positions: patch is facing the liquid (front loading) and ground is facing the liquid (back loading).

The antenna is also experimentally characterized using the DASY-5 system. A series of experimental field measurements of the designed antenna is performed using the DASY5 system. A map of SAR value at the 1800 MHz and 0.5 W input power is shown in Fig. 9, on a slice that 4-mm away from internal surface of the phantom. The robot is programmed to touch the surface of the phantom and then retreats 4 mm normal to the surface before acquiring one sensor reading, for each pixel. The hot-spot maximum SAR is found to be 2.01 mW/g.

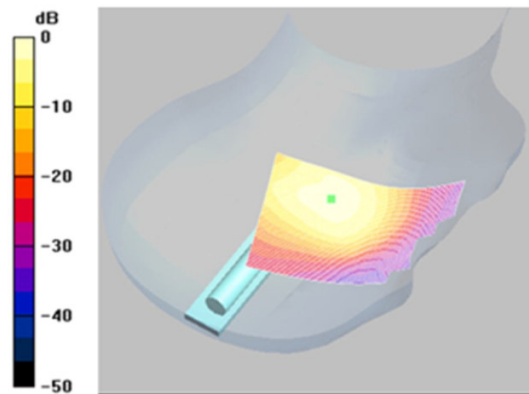


**FIGURE 9.** Experimentally measured SAR on the internal surface of the phantom at 1800-MHz. 0.5-W input power is used. 0-dB corresponds to 2.01 mW/g.

## CONCLUSIONS

A nondestructive evaluation method is developed to characterize the new category of reconfigurable antennas using computational and experimental techniques. The studied antenna is a compact single feed dual-band electronically tunable structure, designed for operation in GSM900/DCS1800 system. A model based on FDTD is performed of the antenna in free space and in proximity to the human head. As the antenna gets in proximity

to the head, a shift in antenna center frequency has been observed depending to antenna orientation with respect to the body. The effect is significant if the antenna patch facing the body and is insignificant whenever the ground is facing the body. This is the ideal normal position of use of mobile handsets. A scheme based on DASY5 scanning system has been implemented to characterize experimentally the SAR values within the human head. Good agreement between simulations and experimental results has been observed. The developed system provides a tool for precise evaluation of radiation doses. It can be used to guide the design of optimum structures of the new class of reconfigurable antennas.

## ACKNOWLEDGEMENTS

This research is supported by King Abdulaziz City for Science and Technology (KACST), Research Grant: AT-26-34.

## REFERENCES

1. J. T. Aberle, et al., *IEEE Antennas Propag. Mag.* **45**, 148-154(2003).
2. A. F. Sheta and M. Alkanhal, *IET Microw. Antennas Propag.* **2**, pp. 274-280 (2008).
3. M. Alkanhal and A. F. Sheta, *Progress Electromag. Research. PIER* **70**, pp. 337-349 (2007).
4. K. L. Virga and Y. R. Samii, *IEEE Trans. Microw. Theory Tech.* **45**, pp. 1879–1888 (2002).
5. D. Peroulis, K. Sarabandi, and L. Katehi, *IEEE Trans. Antennas Propag.* **53**, pp. 645–654 (2005).
6. N. Behdad and K. Sarabandi, *IEEE Trans. Antennas Propag.* **54**, pp. 409–416 (2006).
7. N. Behdad and K. Sarabandi, *IEEE Trans. Antennas Propag.* **54**, pp. 401-408 (2006).
8. A. F. Sheta and S. F. Mahmoud, *IEEE Antennas and Wireless propag. Letters* **7**, pp. 40-42 (2008).
9. H. Okabe and K. Takei, *Proc. IEEE AP-Symp.*, pp. 166-169 (2001).
10. N. C. Karmakar, *IEEE Trans. Antennas Propag.* **52**, pp. 2877–84 (2004).
11. A. W. Preece, “Safety Aspects of Radio frequency Effects in Humans from Communication Devices,” in *Handbook of Antennas in Wireless Communications*, edited by L. C. Godara, CRC Press, 2001.
12. S. F. Cleary, “Cellular Effects of Radio-Frequency Electromagnetic Fields,” in *Biological Effects and Medical Applications of Electromagnetic Energy*, edited by O. P. Gandhi, Prentice Hall, 1990.
13. D. Remondini, et al., *Proteomics* **6**, pp. 4745-4754 (2006).
14. K. S. Yee, *IEEE Trans. Antennas Propag.* **14**, pp. 302-307 (1966).
15. SEMCAD-X package. <http://www.semcad.com>.
16. S. Gabriel, R. W. Lau, and C. Gabriel, *Phys. Med. Biol.* **41**, pp. 2271-93 (1996).
17. DASY5 System, Speag, Zurich, Switzerland. <http://www.speag.com>.



1. **Aberle, J. T., et al.** Reconfigurable antennas for portable wireless devices. *IEEE Antennas and Propagation Magazine*. December 2003, Vol. 45, 6.
2. **Sheta, A. F. and Alkanhal, M.** Compact Dual-Band Tunable Microstrip Antenna for GSM/DCS-1800 Applications. *to appear in IET Antenna and Microwave Propagation*. 2008.
3. **Alkanhal, M. and Sheta, A. F.** A Novel Dual-Band Reconfigurable Square-Ring Microstrip Antenna. *Progress In Electromagnetics Research*. 2007, Vol. PIER 70, pp. 337-349.
4. **Virga, K. L. and Samii, Y. R.** 4. , “Low-profile enhanced-bandwidth PIFA antennas for wireless communications packaging,”, Vol. 45, pp. , . *IEEE Trans. Microwave Theory Tech.* Oct.r 2002, pp. 1879–1888.
5. **Peroulis, D., Sarabandi, K. and Katehi, L.** Design of reconfigurable slot antennas. *IEEE Trans. Antennas Propagat.* Feb. 2005, Vol. 53, pp. 645–654.
6. **Behdad, N. and Sarabandi, K.** Dual-band reconfigurable antenna with a very wide tenability range. *IEEE Trans. Antennas Propagat.* Feb. 2006, Vol. 54, pp. 409–416.
7. —. A varactor-tuned dual-band slot antenna. *IEEE Trans. Antennas Propagat.* Feb. 2006, Vol. 54, pp. 401-408.
8. **Sheta, A. F. and Mahmoud, Samir F.** Compact Tunable Patch Antenna with Wide Tuning Range. *Accepted for publication in IEEE Antennas and wireless propagation letters*. 2008.
9. **Okabe, H. and Takei, K.** Tunable antenna system for 1.9 GHz PCS handsets. *in Proc. IEEE AP-Symp.* 2001, pp. 166-169.
10. **Karmakar, N. C.** Shorting strap tunable stacked patch PIFA. *IEEE Trans. Antennas Propagat.* Nov. 2004, Vol. 52, pp. 2877–2884.
11. **Preece, Alan W.** Safety Aspects of Radio frequency Effects in Humans from Communication Devices. [ed.] Lal Chand Godara. *Handbook of Antennas in Wireless Communications*. : CRC Press, 2001.
12. **Cleary, S.F.** Cellular Effects of Raido-Frequency Electromagnetic Fields. [book auth.] O. P. Gandhi. *Biological Effects and Medical Applications of Electromangetic Energy*. s.l. : Prentice Hall, 1990, p. 339.
13. **Remondini, D., et al.** Gene expression changes in human cells after exposure to mobile phone microwaves. 2006, Vol. 6, pp. 4745-4754.
14. **Yee, Kane S.** Numerical solution of initial boundary value problems involving Maxwell’s equations in isotropic media, vol.14.,. *IEEE Trans. Antennas Propagation*. 1966, Vol. 14, 3, pp. 302-307.
15. **SEMCAD<sup>X</sup>, package.** *SEMCAD<sup>X</sup>*. [www.speag.com](http://www.speag.com).
16. **Gabriel, S., Lau, R. W. and Gabriel, C.** The dielectric properties of biological tissues: III. Parametric models for dielectric spectrum of tissues. *Phys.Med. Biol.* 1996, Vol. 41, pp. 2271-93.
17. **DASY5.** Speag Company. *Zurich, Switzerland*. [Online] [www.speag.com](http://www.speag.com).